Electronic Supplementary Material (ESI) for Green Chemistry.

Hydrothermal saline promoted grafting: A new route to sulfonic acid SBA-15 silica with ultra-high acid site loading for biodiesel synthesis

C. Pirez[b,c*], A. F. Lee[a], J. C. Manayil[a], C.M.A. Parlett, K. Wilson[a*]

[a] European Bioenergy Research Institute, School of Engineering and Applied Sciences, Aston University, Birmingham, B4 7ET, UK

[b] School of Chemistry, Cardiff University, Park Place, Cardiff, CF10 3AT

[c] Present address : UCCS, University of Lille I, 59655 Villeneuve d'Ascq, France

[*]Corresponding author: E-mail: k.wilson@aston.ac.uk

S1 Experimental

S1.1 Catalyst synthesis

<u>SBA-15 synthesis:</u> SBA-15 material was prepared following Zhao's protocol[1]. SBA-15 was prepared from 1.0 g of Pluronic P123 triblock copolymer which was dissolved in 7.5 ml of water and 25 ml of 2M HCl solution (Fisher), stirred at 35 °C. 2.3 ml of TEOS were added to the solution, which was maintained at 35 °C for 24 h under stirring. Then, the mixture was then aged at 80 °C for 24 h. Finally, the solid product was filtered, washed 3 times with deionized water and calcined statically in air at 550 °C for 6 h.

<u>One-pot synthesis:</u> $PrSO_3H$-SBA-15 was synthesized by co-condensation method, according to the protocol of Margolese[2]. 4 g of Pluronic 123 was first dissolved with 125 cm^3 of 2 M HCl at 40 °C. Subsequently, 8.2 ml of tetraethylorthosilicate (TEOS) was added, and after 45 min reaction, 0.76 mL of 3-mercaptopropyl-trimethoxysilane (MPTMS) and 3.8 ml of H_2O_2 were added simultaneously and the solution was stirred for 24 h. The mixture was then aged at 100 °C for a further 24 h, and the resulting solid filtered, washed three times with water and finally dried overnight at room temperature (RT). Template was extracted by MeOH reflux method. *The acid catalyst was called $PrSO_3H$-SBA-15-OP.*

<u>Grafting sulfonic groups in toluene:</u> SBA-15 was functionalized with propylsulfonic acid by standard post-grafting method. 1 g SBA-15 was added to a solution containing 1 ml of mercaptopropyl trimethoxysilane (MPTMS 95%, Alfa Aesar) in 30 ml of toluene (Fisher 99%). The suspension was then refluxed at 130 °C under stirring for 24 h, after which the resulting thiol-functionalized solid was filtered, washed three times with methanol (Fisher 99%) and dried at RT. Thiol groups were converted

into -SO_3H by mild oxidation with 30 ml of 30 % hydrogen peroxide (Sigma-Aldrich) by continuous stirring at room temperature for 24 h. The sulfonated solid product was subsequently filtered, washed three times with methanol and dried at RT. *The acid catalyst was called PrSO$_3$H/SBA-15-Tol.*

Grafting sulfonic groups in H_2O/NaCl solution: 1 g SBA-15 was mixed in 30ml H_2O with (or without) NaCl for 15min. Then, 1ml of MPTMS is added. The suspension was then refluxed at 100 °C under stirring for 24 h, after which the resulting thiol-functionalized solid was filtered, washed three times with H_2O and dried at RT. Thiol groups were converted into -SO_3H by mild oxidation with 30 ml of 30 % hydrogen peroxide (Sigma-Aldrich) by continuous stirring at room temperature for 24 h. The sulfonated solid product was subsequently filtered, washed three times with methanol and dried at RT. *The acid catalyst was called PrSO$_3$H/SBA-15-H$_2$O-X* (where X correspond to the amount of NaCl mg used for the grafting process)

S1.2 Characterization

All the acid catalysts were fully characterized. Nitrogen adsorption-desorption was measured using a Quantachrome Nova 2000e porosimeter using NOVAWin software. Samples were degassed at 120 °C for 2 h before analysis by N_2-adsorption at −196 °C. BET surface areas were calculated over the relative pressure range 0.01–0.2. Pore diameters and volumes were calculated applying the BJH method to the desorption isotherm for relative pressures >0.35. Low-angle powder XRD patterns were recorded on a PANalytical X'pertPro diffractometer fitted with an X'celerator detector and Cu Kα (1.54 Å) source calibrated against a Si standard (PANalytical). Low angle patterns were recorded for $2\theta = 0.3–6°$ with a step size of 0.01°.

TEM pictures were obtained with a JEOL 2100 transmission electron microscope operated at 200 kV, with images recorded by a Gatan Ultrascan 1000XP digital camera. Image analysis was undertaken using ImageJ software. XPS was performed using a Kratos Axis HSi X-ray photoelectron spectrometer fitted with a charge neutraliser and magnetic focusing lens employing Al Kα monochromated radiation (1486.6 eV). Surface elemental analysis was undertaken on Shirley background-subtracted spectra applying the appropriate instrument and element-specific response factors. Spectral fitting was conducted using CasaXPS version 2.3.14, with binding energies corrected to the C 1s peak at 284.8 eV and high-resolution C 1s, O 1s, S 2p and Si 2p XP spectra fitted using a common Gaussian/Lorentzian peak shape. Errors were estimated by varying the Shirley background subtraction procedure across reasonable limits and re-calculating fits. Thermogravimetric analysis (TGA) was performed using a Stanton Redcroft STA780 thermal analyzer on ∼10–20 mg samples under helium ($20\ cm^3.min^{-1}$ total flow) during heating at 10 °C. min^{-1} between 20 °C and 800 °C. Acid site titration were made via NH_3 pulse chemisorption using a Quantachrome ChemBET 3000 instrument at 100 °C on samples degassed at 150 °C. After NH_3 saturation into the catalysts, TPD-NH_3 was performed at 100^oC up to 800^oC, followed by Mass spectrometer (m/z=16). DRIFT spectra were obtained using a Nicolet Avatar 370 MCT with Smart Collector accessory, mid/ near infrared source and mercury cadmium telluride (MCT-A) photon detector at −196 °C (liquid N_2). Samples were diluted with KBr powder (5 wt% in KBr) for analysis and then loaded into an environmental cell and subjected to additional drying under vacuum at 200 °C for 2 h prior to measurements to remove moisture physisorbed during air exposure. All spectra were normalized from peak observed at 1850cm-1 for better visualization of changing in silanol region. ^1H, ^{13}C, and ^{29}Si MAS-NMR was conducted at the EPSRC UK National Solid-state NMR Service at Durham using a Varian VNMRS 400 instrument. Spectra were acquired under Cross polarisation (CP) & direct excitation (DE) using tetramethylsilane as a reference.

S1.3 Esterification and transesterification reaction

Esterification reactions were performed under stirred batch conditions at atmospheric pressure in a Radley's carousel reaction station using a 25 mm diameter glass reactor vessel. 10 mmol of palmitic acid was reacted at 60 °C in 12.5 ml methanol (molar ratio MeOH:acid = 30) with 50 mg catalyst and 0.6 ml (2.5mmol) of dihexylether added as an internal standard. Reaction profiles were obtained via periodic sampling and off-line GC analysis, with product calibration curves used to verify mass balances (all >98 %). All catalytic profiles are an average of two separate runs with 3 injections per sample. Esterification was monitored using a Varian 450-GC equipped with a CP-Sil 5 CB 15 m × 0.25 mm × 0.25 µm capillary column. Dichloromethane was used to dilute samples for GC analysis. Turnover frequencies (TOF) were determined from the linear portion of the initial reaction rate profile for conversions below 25%, normalized to the acid site concentration determined from NH_3 titrations.

Glyceryl palmitate transesterification was made in 50ml ACE™ glass pressure flask under stirring at 80^oC. 10 mmol of Tripalmitate (C16) was dissolved in mixture of 12.5 ml methanol with 12.5ml butanol added to aid solubilty. Then, 50 mg of catalyst and 0.3 ml of dihexylether was added as an internal standard. Sampling was made after 24h of reaction. Tripalmitate transesterification was monitored using Varian 450-GC equipped with a 1079 programmable direct cooled on-column injector and Phenomenex capillary column ZB-1HT Inferno 15m x 0.53mm x 0.15µm. The proportion of methyl and butyl ester produced were the same for the different catalysts tested (75% methyl ester and 25% butyl ester).

S2 Results and Discussion

Table S1 shows how the physical parameters of grafted sulfonic acid catalysts varies as a function of [NaCl] from x=0-1000 mg. Addition of up to 200mg of NaCl results in a decrease in surface area attributed to an increase of grafting efficiency as evidenced by the S content and acid site loading. Further increases in [NaCl] inhibit silane grafting with both a decrease in S and acid site loading observed along with a concomitant increase in surface area. The N_2-isotherms also change as a function of [NaCl] with the BJH plot showing a bimodal distribution (**Fig S1**), except for the catalyst $PrSO_3H$/SBA-15-200, where NaCl concentration is optimal. NaCl clearly influences the grafting on the silica surface and it appears we need an optimal concentration of NaCl to achieve monolayer coverage of -$PrSO_3H$ on the surface.

Table S1. Textural properties of $PrSO_3H$/SBA-15 with different NaCl concentration in the solution

NaCl (mg)	**NaCl/SiOH$_{surface}$ molar ratio**[a]	**BET**[b] **/m².g^{-1}**	**Vp /cm^3.g^{-1}**	***BJH* pore diameter**[c] **/nm**	**Plane spacing**[d] **/nm**	**Unit cell parameter**[e] **/nm**	**Wall thickness**[f] **/nm**	**Surf. S content**[g] **/wt%**	**Acid capacity**[h] **/mmol$_{H+}$.g^{-1}**	**Sulfur density /nm^{-2}**	**Acid density /nm^{-2}**
0	0	491	0.59	3.6, 4.6	8.4	9.7	4.9	4.3	1.6	1.6	2
100	0.6	412	0.50	3.6, 4.5	8.3	9.6	5.9	4.7	1.8	2.1	2.5
200	1.1	323	0.44	3.6, 4.5	8.7	10	6.3	5.3	2.2	2.5	3.5
500	2.8	409	0.47	3.6, 4.5	8.4	9.7	6.1	5	2	2.3	3.2
1000	5.7	434	0.51	3.6, 4.5	8.4	9.7	6	4.8	1.9		2.6

[a] SiOH in SBA-15 calculated from TGA analysis, [b] From BET equation. [c] Analyzed from the desorption branch. [d] From Braggs law using (100) plane, [e] a0 = (2d100)/√3, [f] a_0 - pore diameter, [g] Surface S content from XPS. [h] Based on NH_3 pulse titration

Table S2. Summary of deconvoluted Qn and Tm species in ^{29}Si MAS-NMR for SBA-15 and Pr-SO_3H/SBA-15 catalysts prepared via, one-pot, toluene, and H_2O/NaCl grafting routes.

Samples	**Q4 /%**	**Q3 /%**	**Q2 /%**	**T3 /%**	**T2 /%**	**Tm/(Tm+Qn) /%**
SBA-15	57.8	31.4	10.8	-	-	0
$PrSO_3H$-SBA-15-OP	55.5	32	3.4	7.5	1.5	9
$PrSO_3$/SBA-15-TOL	51.5	30	8.4	2.3	1.8	4.1
$PrSO_3H$/SBA-15-0	45	29.4	4.9	14	6.8	17.7
$PrSO_3H$/SBA-15-200	44.8	26.9	2.6	19	6.6	24.3

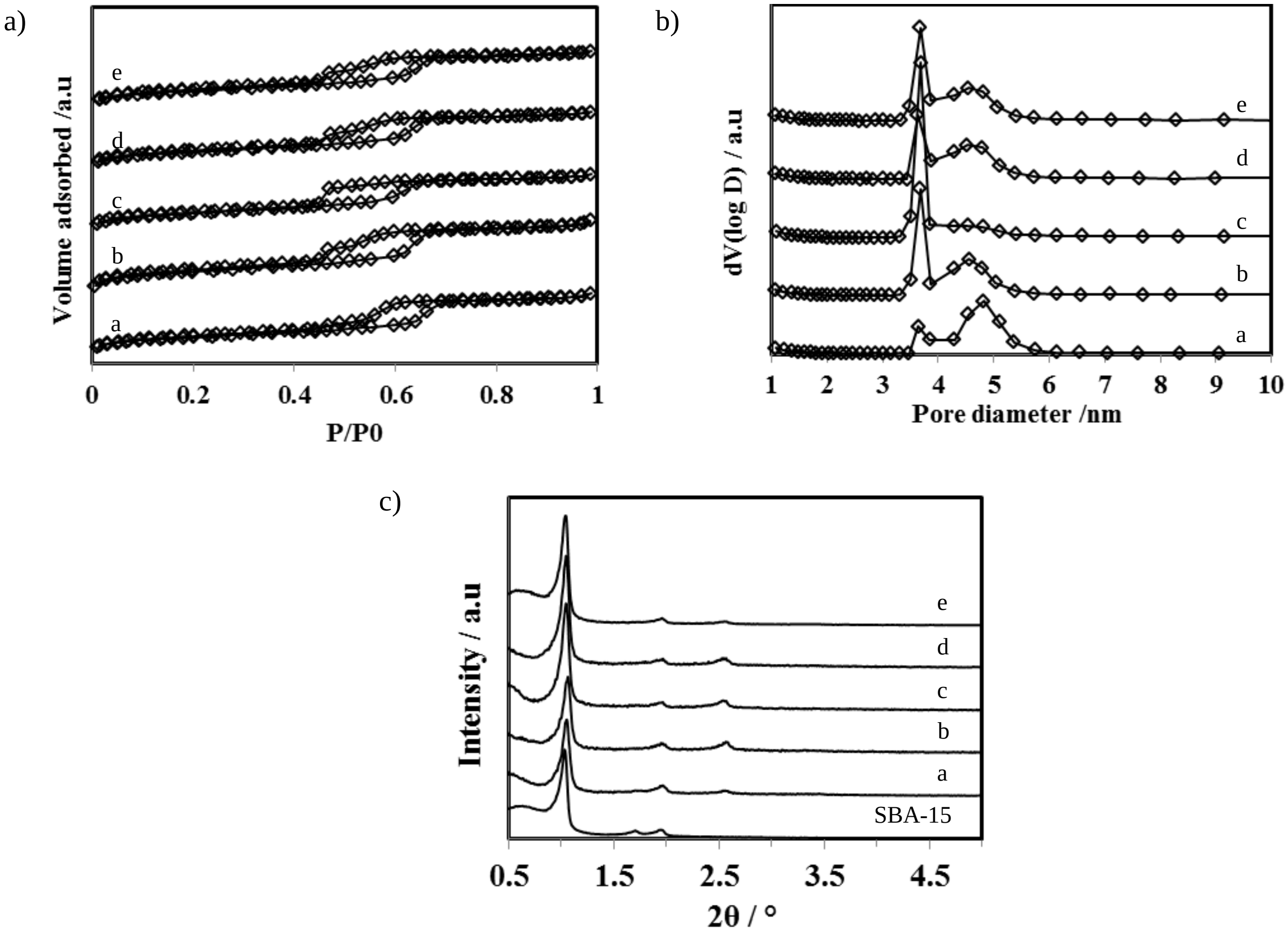

Fig. S1. a) N_2 isotherms b) BJH pore size distribution and c) low angle XRD of $PrSO_3H$/SBA-15 prepared with different NaCl concentration; a-x=0, b-x=100, c-x=200, d-x=500 and e-x=1000 mg. g^{-1} SiO_2

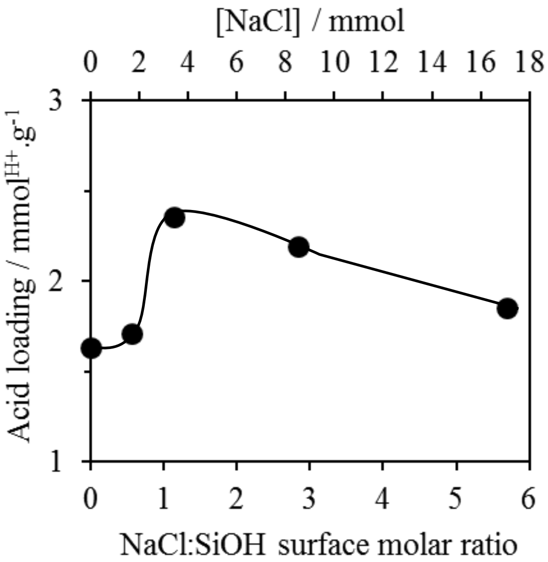

Fig. S2. Variation in acid site loading of $PrSO_3H$/SBA-15 prepared with different NaCl concentration showing correlation with NaCl:SiOH surface ratio. [SiOH] determined to be 3 mmol.g^{-1} as calculated from TGA on the parent SBA-15

The correlation between acid site and sulfur loading shown in **Figure S3** also suggests complete oxidation of thiol groups and good accessibility of sulfonic acid groups in all the catalysts synthetized to NH_3. The absence of disulfide groups (-Pr-S-S-Pr-) after oxidation in H_2O_2 was verified by ^{13}C MASNMR, thermogravimetric analysis and XPS. The absence of any features at 41 and 23 ppm in the ^{13}C MASNMR (**Figure S4**) indicates that disulfide are not formed in this synthesis. **Figure S5** shows the TGA, from which the absence of any weight loss <350°C which would be attributed to thiol (–SH) or disulfide (–S-S-) decomposition[3,4] also supports this observation. The weight loss observed 400 - 600°C corresponds to decomposition of propyl sulfonic acid groups.[5] -Pr–SH and -Pr–S-S-Pr- groups on the surface are not observed by XPS analysis as well (Fig.S5B).

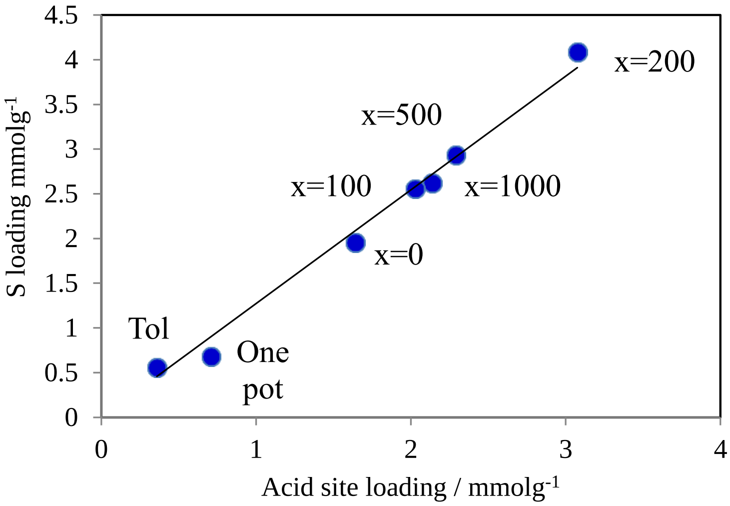

Fig. S3: Correlation between sulfur density and acid site density for all sulfonic acid catalyst prepared as a function of [NaCl] shown as x=0-1000 mg.g^{-1}(SiO_2), along with conventional toluene grafting and one-pot co-condensation methods.

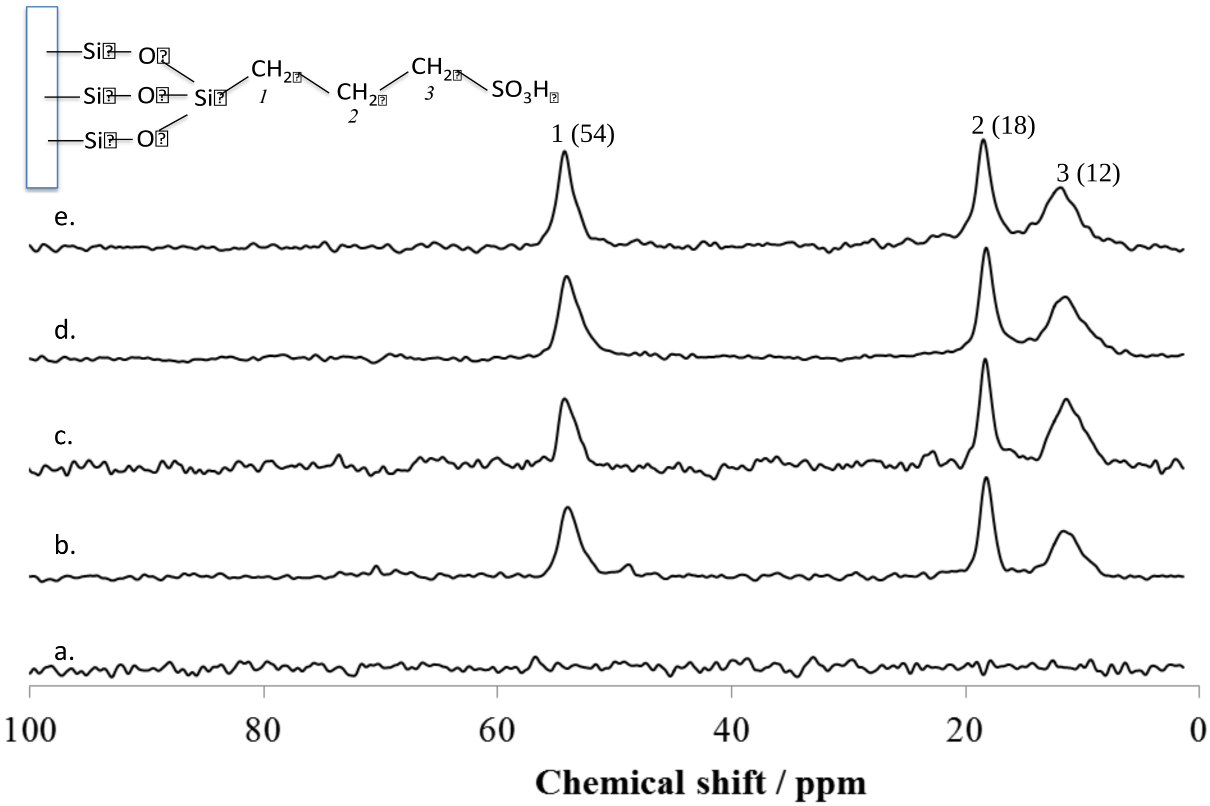

Fig.S4. ^{13}C MAS NMR spectra of SBA-15 functionalized with propylsulfonic acid ; a-SBA-15, b-PrSO$_3$H-SBA-15-OP, c-PrSO$_3$H/SBA-15-Tol, d-PrSO$_3$H/SBA-15-0, e-PrSO$_3$H/SBA-15-200

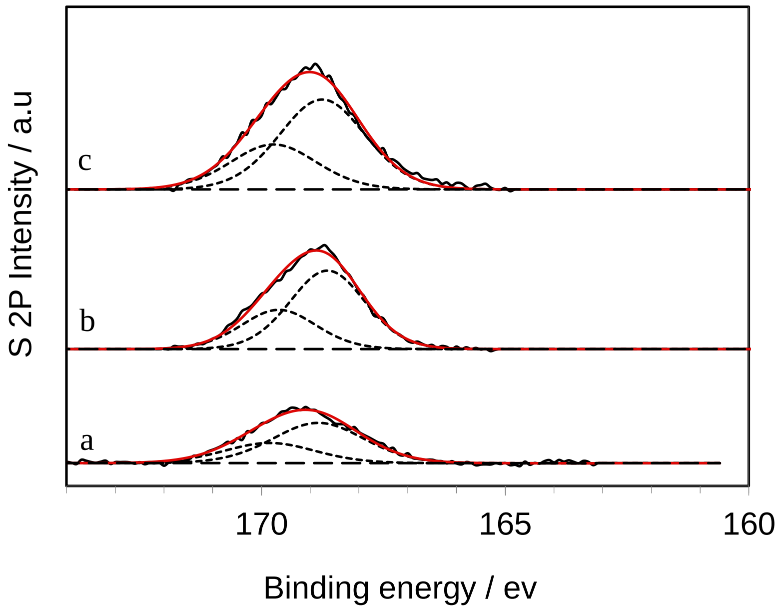

Fig. S5. S2p spectra of mesoporous acid catalysts prepared (Background-subtracted and fitted); a- PrSO$_3$H/SBA-15-Tol, b-PrSO$_3$H/SBA-15-OP, c- PrSO$_3$H/SBA-15-200

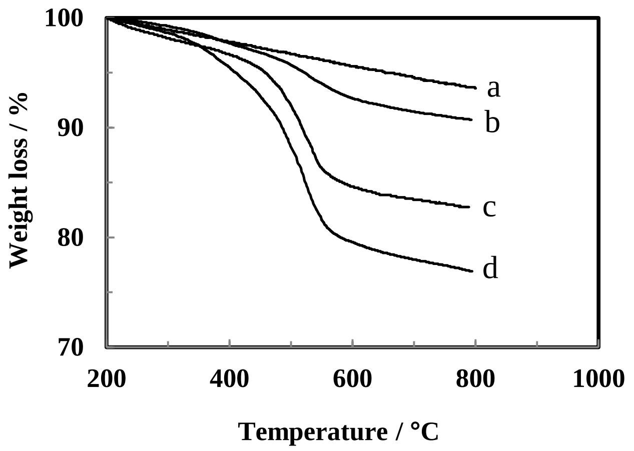

Fig. S6. TGA. a- SBA-15, b-$PrSO_3H$/SBA-15-Tol, c-$PrSO_3H$-SBA-15-OP, d-$PrSO_3H$/SBA-15-200

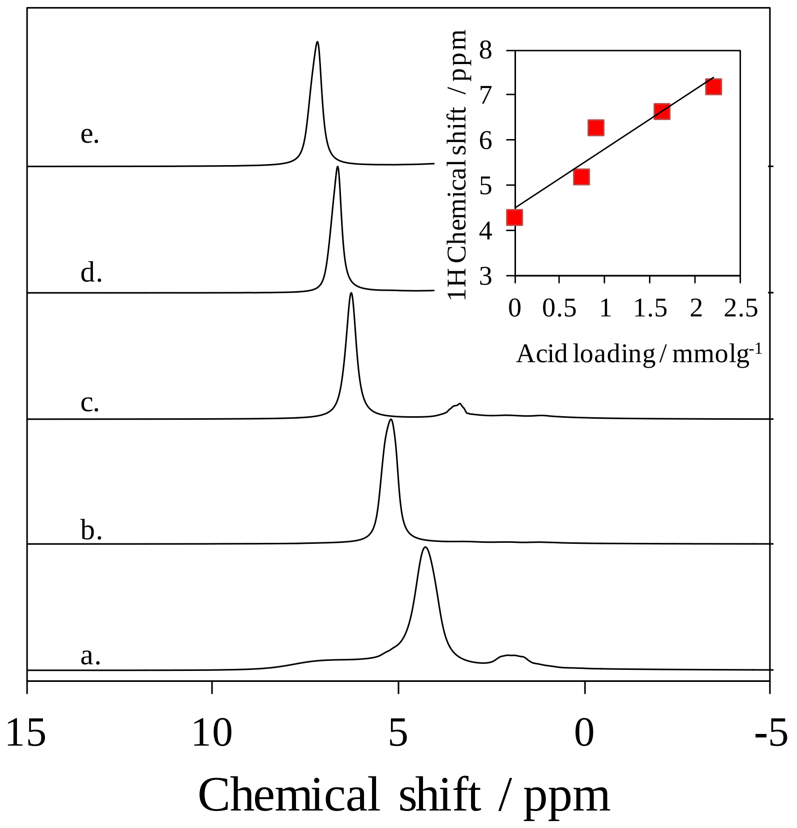

Fig. S7 1H MAS NMR spectra of SBA-15 functionalized with propylsulfonic acid a-SBA-15, b-$PrSO_3H$/SBA-15-Tol, c-$PrSO_3H$-SBA-15-OP, d-$PrSO_3H$/SBA-15-0, e-$PrSO_3H$/SBA-15-200.

The acidic properties of all materials was determined NH_3 pulse titration ($mmol_{H+}.g^{-1}$) with acid site loadings for $PrSO_3H$/SBA-15-200 found to be 5 and 2.4 times higher compared to $PrSO_3H$/SBA-15-Tol and $PrSO_3H$/SBA-15-OP. NH_3 temperature program desorption of the three catalysts show a shift to higher temperature (between 150-400°C) when the functionalization method is changed, indicating acid strength increases in the order: $PrSO_3H$/SBA-15-200 > $PrSO_3H$-SBA-15-OP > $PrSO_3H$/SBA-15-Tol (**Fig S8**), and is in good agreement with ^1H MAS-NMR. An increase in acid strength can arise due to the cooperative effects of acid sites through formation of hydrogen bonding between pair of adjacent sites, which stabilizes anion formed after deprotonation of acid group.[5] Desorption observed above this temperature is attributed to sulfonic acid decomposition.[6]

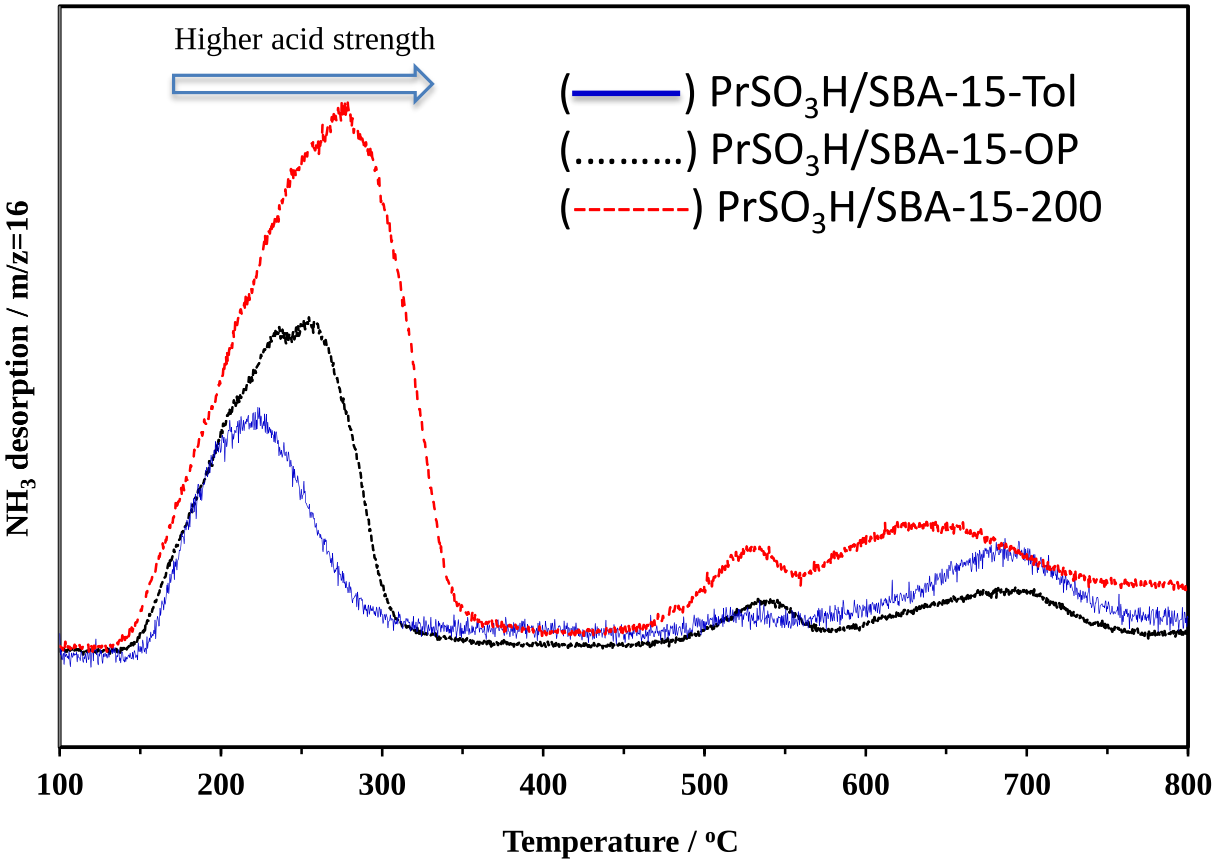

Fig. S8. Temperature programm desorption of NH_3 (m/z=16) over $PrSO_3H$/SBA-15-Tol, $PrSO_3H$/SBA-15-H_2O-200 and $PrSO_3H$/SBA-15-OP. Peak areas are normalised per gram of solid acid catalyst.

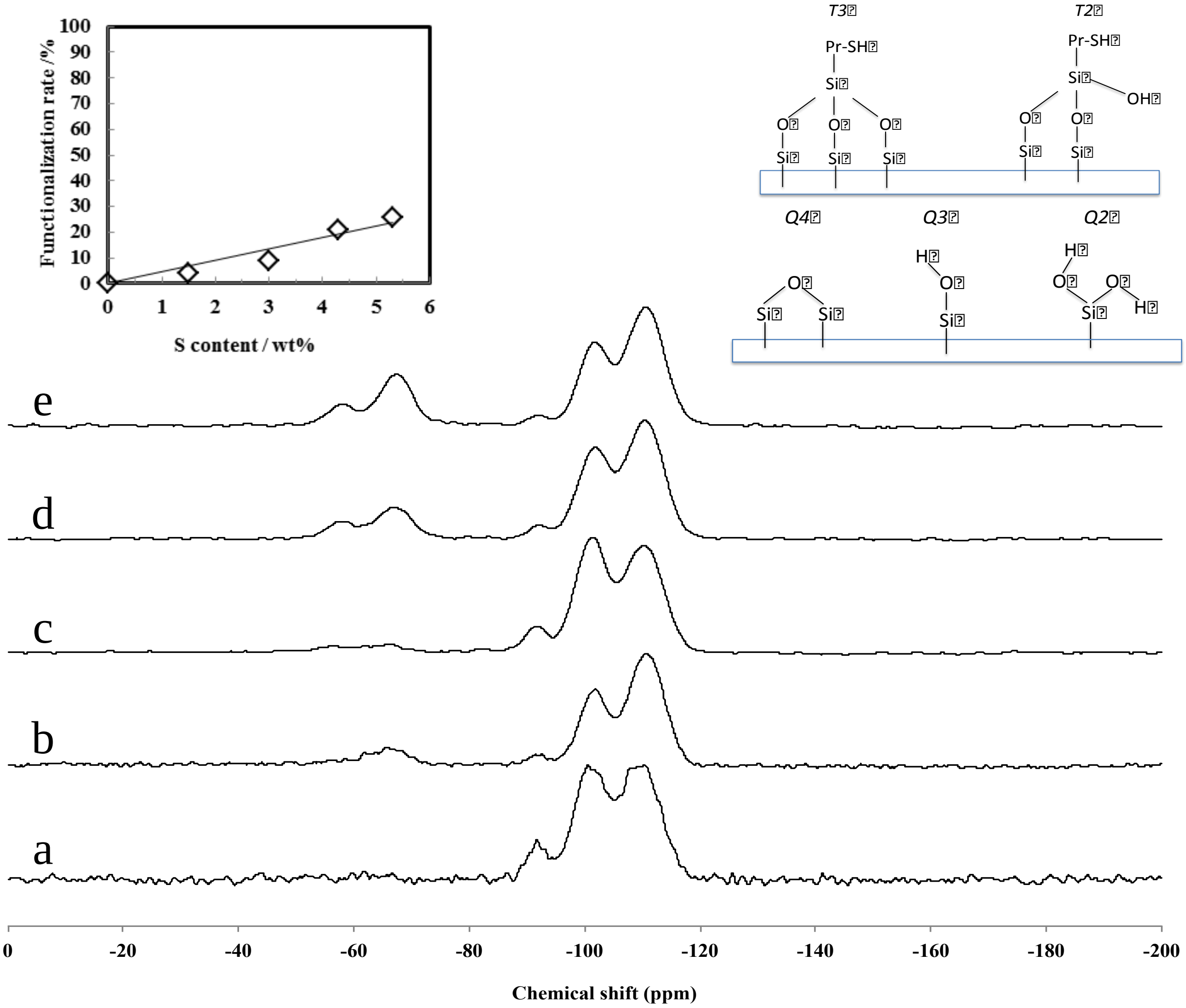

Fig S9 ^{19}Si MAS NMR spectra showing evolution Tm and Qn species for (i) SBA-15, (ii) PrSO$_3$H-SBA-15-OP, (iii)Tol-PrSO$_3$H/SBA-15, (iv) PrSO$_3$H/SBA-15-0 and (v) PrSO$_3$H/SBA-15-200. Inset shows structures for Tm and Qn surface species. Signals at -91, -101, and -110 ppm, correspond to Q2, Q3 and Q4 species for the support respectively, while those at -66 and -58 ppm, are attributed to T3 and T2 coordinated organosilanes.

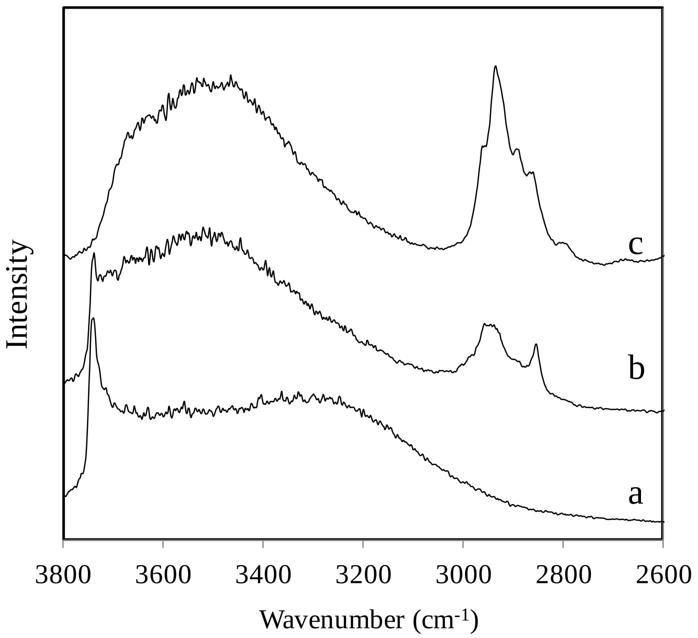

Fig. S10. DRIFTS spectra; a-SBA-15, b-$PrSO_3H$/SBA-15-Tol and c-$PrSO_3H$/SBA-15-200

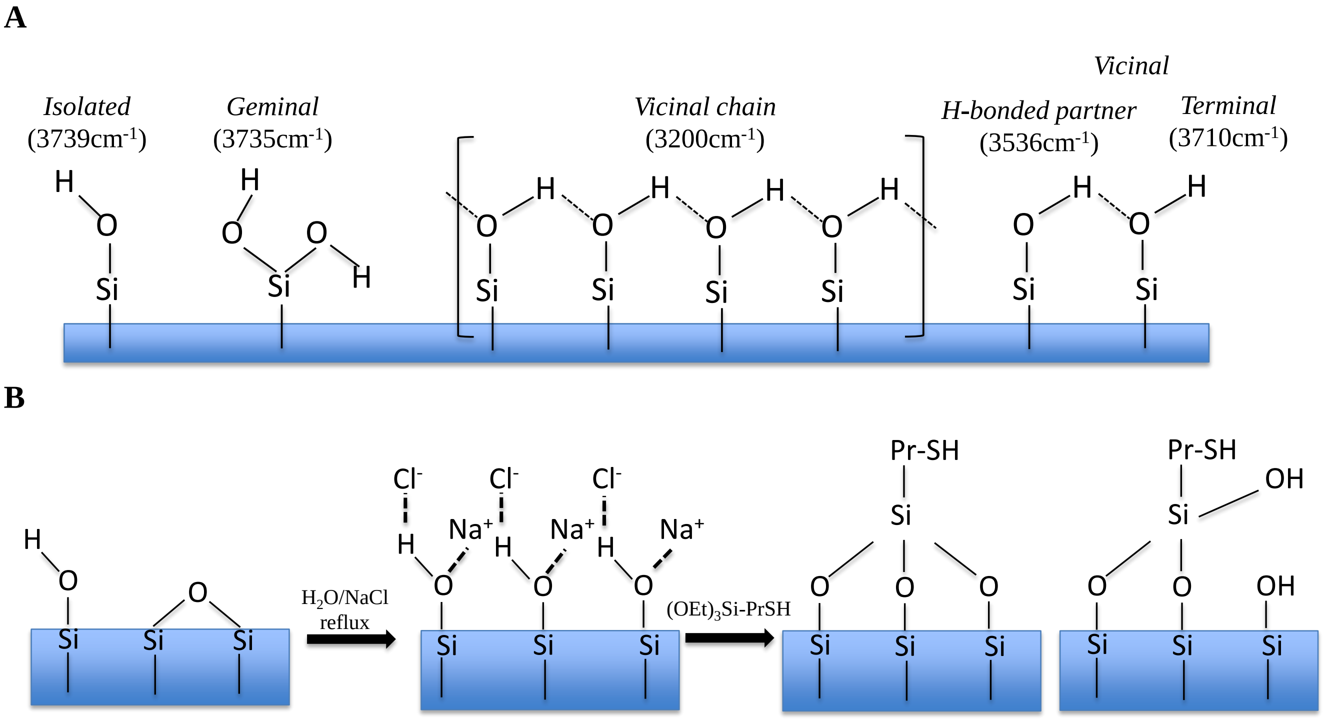

Scheme S1. A) Assignment of DRIFTS mode of hydroxyl groups; B) Possible role of H_20/NaCl in activating siloxane bridges for grafting.

Fig. S11A shows N_2 isotherms of SBA-15, $PrSO_3H$/SBA-15 after grafting (in toluene and H_2O/NaCl mixture) and by one pot synthesis. Both the parent support and derivatised catalysts exhibit Type IV isotherms with H1 hysteresis loops, characteristic of open cylindrical pores. BJH pore size distributions (**Fig. S11B**) show after grafting in toluene the pore distribution is similar to SBA-15. However, after grafting in H_2O/NaCl, the isotherms shift to lower partial pressure indicating narrower pore diameter. The observed widening of the hysteresis loop suggests there may be some narrowing of the pore openings following grafting in H_2O/NaCl.[30]

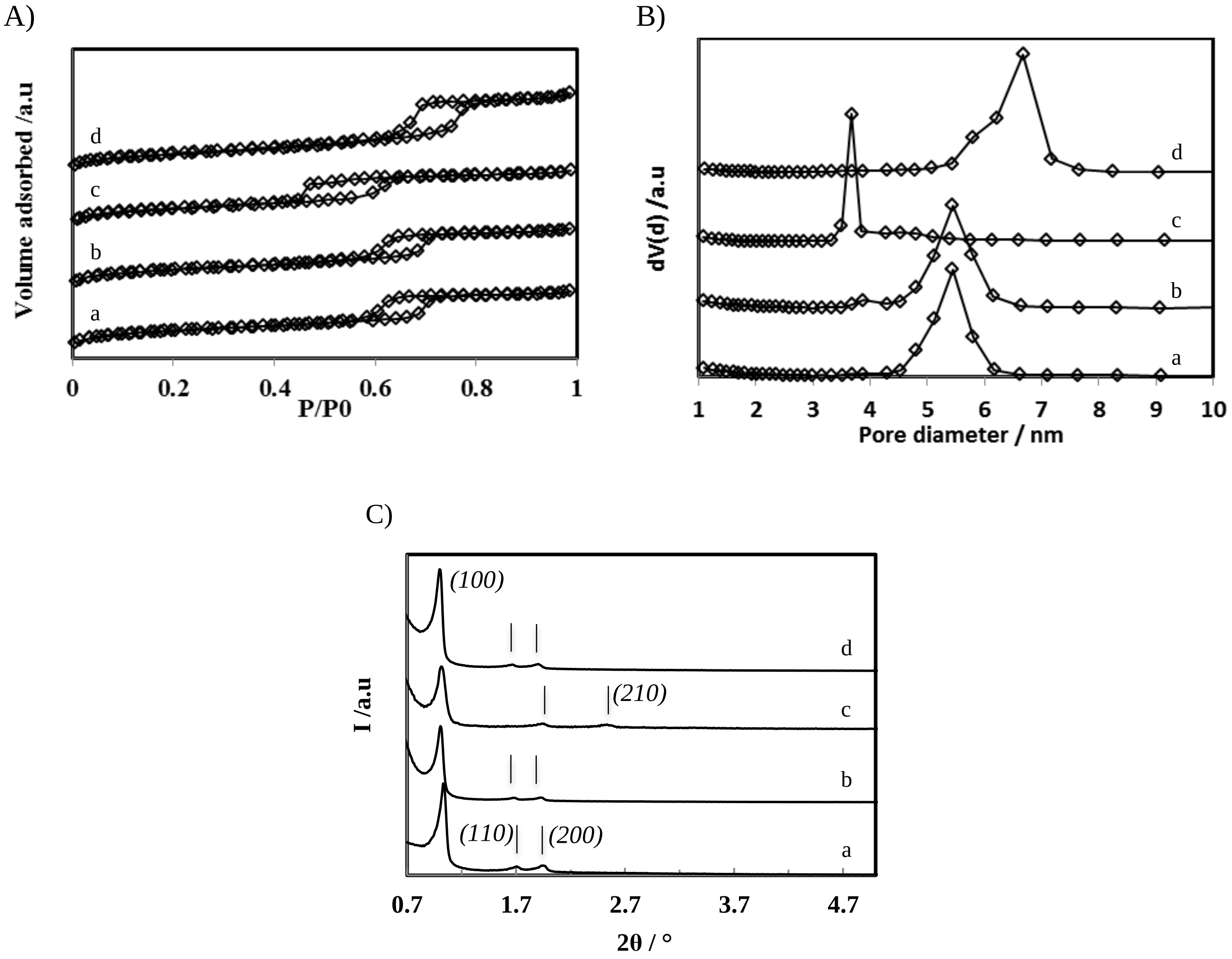

FigS11. A) N_2 adsorption isotherms; B) BJH pore size distribution; and C) low angle XRD for a) calcined SBA-15; b) $PrSO_3H$/SBA-15-Tol; c) $PrSO_3H$/SBA-15-H_2O-200 and d)-$PrSO_3H$-SBA-15-OP.

Low angle XRD patterns (**Fig. S11C**) confirm retention of the p6mm hexagonal structures for SBA-15, $PrSO_3H$/SBA-15-Tol, $PrSO_3H$-SBA-15-OP with typical d_{100}, d_{110}, and d_{200} planes observed. The presence of the extra d_{210} plane in $PrSO_3H$/SBA-15-H_2O-200 is similar to reports for SBA-15 following treatment in boiling H_2O, NH_3 or HF solution.[7] According to Zhao et al, this d_{210} is expected for materials with p6mm hexagonal symmetry,[1] and is often observed in XRD patterns of MCM-41,[8] which is more structured material than SBA-15. Thus we can infer that the observation of the d210 diffraction line for $PrSO_3H$/SBA-15-H2O-200 is a reflection of improved structural order following sulfonation. Loss of the d110 reflection is however intriguing, but has been reported to be very sensitive to the changes in pore width:unit cell ratio;[9] thickening of the walls on high density grafting could account for this observation.

Table S3 summarises physical and chemicals properties of SBA-15 and $PrSO_3H$/SBA-15 catalysts which shows the surface area of $PrSO_3H$/SBA-15-Tol and $PrSO_3H$-SBA-15-OP decreases by ~30% due to anchoring or incorporation of $–PrSO_3H$ groups. The surface area of $PrSO_3H$/SBA-15-200 decreases by ~71%, which we attribute to the high sulfonic acid coverage and loss of microporosity upon treatment in boiling water as reported by Galarneau and al. who demonstrated a 50% of surface area in SBA-15 material.[10] This decrease in surface area is attributed re-deposition of solubilized silica into stable crevices of micropores leading to restructuring of the SBA-15 walls in water and loss of microporosity. Overall the use of H_2O/NaCl as a grafting media result in an increase in sulfur by ~3.5 times compared to conventional grafting in toluene.

Table S3. Summary of physical properties of SBA-15 and Pr-SO_3H/SBA-15 catalysts prepared via one-pot, toluene, and optimum H_2O/NaCl grafting routes.

Materials	BET[a] /$m^2.g^{-1}$	Vp /$cm^3.g^{-1}$	*BJH* pore diameter[b] /nm	Plane spacing[c] /nm	Unit cell parameter[d] /nm	Wall thickness[e] /nm	Surf. S content[f] /%	Acid capacity[g] /$mmol_{H+}.g^{-1}$	Sulfur density /nm^{-2}	Acid density /nm^{-2}
SBA-15	1130	1.2	5.4	8.6	9.9	4.5	-	-	-	-
Pr-SO_3H/SBA-15-Tol	787	0.87	5.4	8.8	10.1	4.8	1.5	0.74	0.36	0.56
Pr-SO_3H/SBA-15-200	323	0,44	3.7	8.7	10	6.3	5.3	2.2	2.5	3.2
Pr-SO_3H-SBA-15-OP	797	1,55	6.7	9.5	11	4.3	3	0.9	0.71	0.68

[a]From BET equation. [b]Analyzed from the desorption branch. [c]From Braggs law assuming that the peak corresponds to the (100) plane, [d]$a0 = (2d100)/\sqrt{3}$, [e]a0 - pore diameter, [f]Surface S content from XPS. [g]Based on NH_3 pulse titration

To confirm structure of $PrSO_3H$/SBA-15-H_2O-200, TEM analysis has been performed and compared with SBA-15 silica support and the others sulfonated catalysts (**Fig. S12**). SBA-15, $PrSO_3H$/SBA-15-Tol and $PrSO_3H$-SBA-15-OP all show ordered materials with long channels, in accord with XRD analysis.

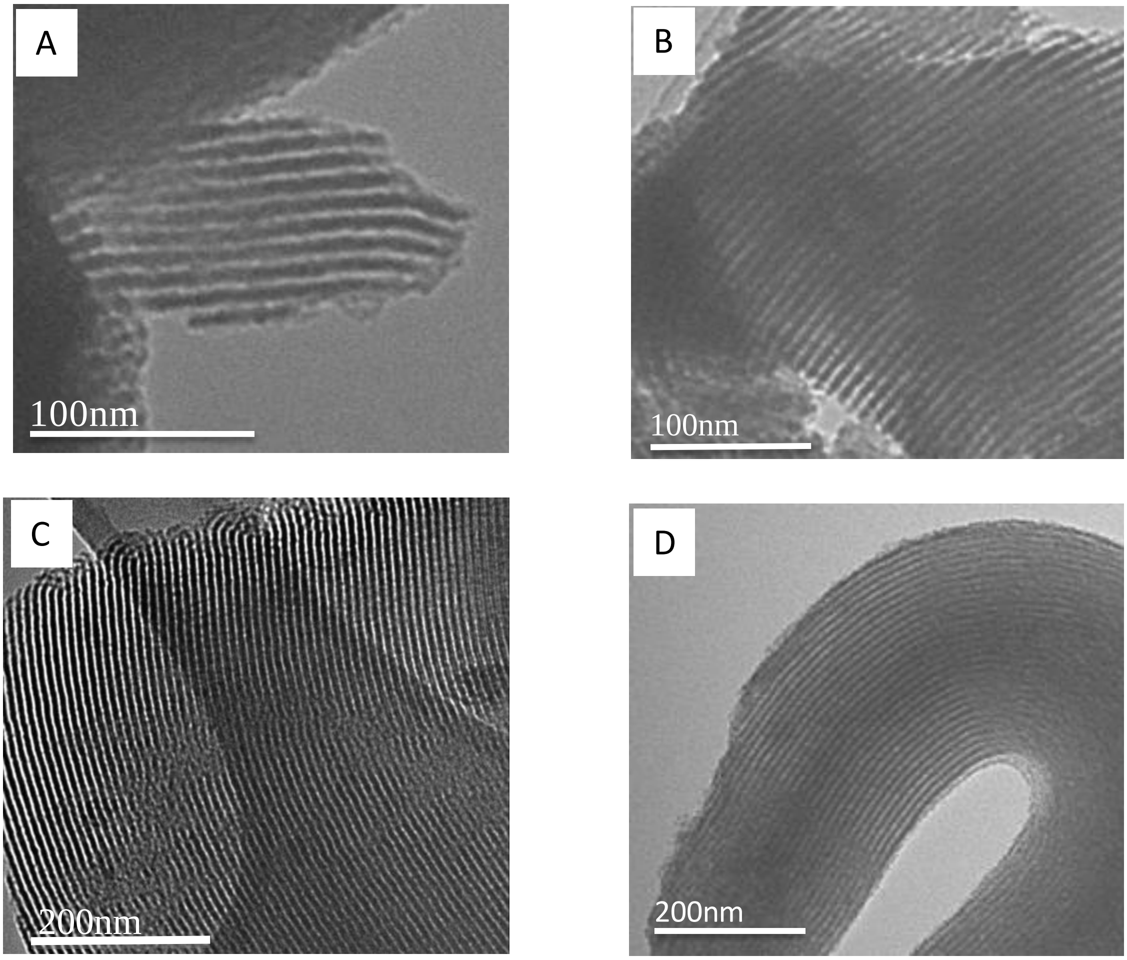

Fig. S12. TEM pictures of prepared $PrSO_3H$/SBA-15; a- SBA-15, b-$PrSO_3H$/SBA-15-Tol, c-$PrSO_3H$/SBA-15-H_2O-200, d-$PrSO_3H$/SBA-15-OP

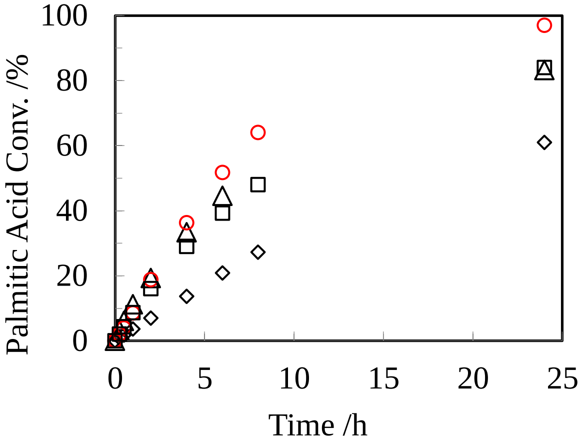

Fig. S13. Palmitic acid conversion versus time; (◇) $PrSO_3H$/SBA-15-Tol, (□) $PrSO_3H$-SBA-15-OP, (○) $PrSO_3H$/SBA-15-200, (△) Amberlyst-15

Table S4. Details of activities in esterification and transesterification using the different sulfonic catalysts prepared

	Functionalization method	**TON**
TG4 (60°C)*	Toluene	67
	X=200	77
	One Pot	56
TG16 (80°C)*	Toluene	8
	X=200	18
	One Pot	12

***Triglyceride reaction was performed in pressure flask/sampling after 24h.**

1. D. Zhao, J. Feng, Q. Huo, N. Melosh, G. H. Fredrickson, B. F. Chmelka and G. D. Stucky, *Science*, 1998, **279**, 548-552.
2. D. Margolese, J. A. Melero, S. C. Christiansen, B. F. Chmelka and G. D. Stucky, *Chemistry of Materials*, 2000, **12**, 2448-2459.
3. J. Aguado, J. M. Arsuaga and A. Arencibia, *Microporous and Mesoporous Materials*, 2008, **109**, 513-524.
4. P.-J. Chiu, S. Vetrivel, A. S. T. Chiang and H.-M. Kao, *New Journal of Chemistry*, 2011, **35**, 489-494.
5. I. K. Mbaraka and B. H. Shanks, *Journal of Catalysis*, 2006, **244**, 78-85.
6. S. Sreevardhan Reddy, B. David Raju, V. Siva Kumar, A. H. Padmasri, S. Narayanan and K. S. Rama Rao, *Catalysis Communications*, 2007, **8**, 261-266.
7. S. A. Kozlova and S. D. Kirik, *Microporous and Mesoporous Materials*, 2010, **133**, 124-133.
8. J. S. Beck, J. C. Vartuli, W. J. Roth, M. E. Leonowicz, C. T. Kresge, K. D. Schmitt, C. T. W. Chu, D. H. Olson and E. W. Sheppard, *Journal of the American Chemical Society*, 1992, **114**, 10834-10843.
9. S. Pikus, L. A. Solovyov, M. Kozak and M. Jaroniec, *Applied Surface Science*, 2007, **253**, 5682-5687.
10. A. Galarneau, M. Nader, F. Guenneau, F. Di Renzo and A. Gedeon, *The Journal of Physical Chemistry C*, 2007, **111**, 8268-8277.